

Raman microprobe spectra of spin-oriented and drawn filaments of poly(ethylene terephthalate)

Fran Adar

Instruments SA, Metuchen, NJ 08840, USA

and Herman Noether

Textile Research Institute, Princeton, NJ 08542, USA

(Received 23 November)

Polarized Raman spectra of single filaments of spin-oriented and drawn fibres of poly(ethylene terephthalate) were recorded. Various Raman bands and their intensities correlated with (1) conformation of the glycol linkage, (2) orientation of the chains, and (3) crystallinity. Because the degrees of crystallinity and orientation were known from X-ray diffraction, density and optical birefringence, it became possible to identify features of the Raman spectra which correlated with each of the effects noted above. The degree of orientation, as a function of take-up speed or draw ratio, was correlated with the intensity ratios of the various polarization components. The appearance and increases in intensity of bands due to *trans* glycol conformations and the disappearance of the *gauche* bands with increasing orientation could be followed readily. It appears that many of the Raman bands earlier assigned to crystallinity in PET actually represent the *trans* conformation of the glycol group as is also observed in i.r. spectra. This conclusion is based on the observation that in spin-oriented amorphous materials the *trans* conformation bands increase in intensity with increasing birefringence. Also an amorphous highly oriented fibre shows these same *trans* conformation bands with high intensity. On the other hand, the width of the carbonyl band, which is the classical indicator of the amorphous or crystalline character of PET, confirmed the amorphous nature of this sample. In conclusion, by monitoring appropriate features of the Raman spectra of spin-oriented and drawn fibres, we have been able to confirm that orientation can occur independently of crystallization in PET.

(Keywords: poly(ethylene terephthalate); spin orientation; filaments; Raman microprobe; crystallization; ethylene glycol conformation)

INTRODUCTION

X-ray diffraction (XRD) studies¹ of poly(ethylene terephthalate) (PET) show that in the crystalline form, molecular chains are aligned so that the glycol units between aromatic rings are in the all-*trans* conformation, the carbonyl units are co-planar with the rings, and all aromatic rings are parallel but with each successive unit slightly displaced in a direction normal to the ring (see Figure 1). In principle, all of the C–C and C–O bonds between the aromatic groups allow some rotational freedom, which may occur in non-crystalline material. Our present understanding of the crystallization process assumes that the ethylene glycol units align in the all-*trans* conformation and that the carbonyl groups rotate into the aromatic planes. While X-ray diffraction can quantify the degree of orientation of crystalline material only, optical birefringence can measure total orientation²—that of both amorphous and crystalline material. While it is possible to prepare samples with close to 100% uniaxial orientation (the polymer axis almost parallel to the macroscopic axis and no orientation order perpendicular to this axis), the most highly crystallized samples are only approximately 50% crystalline. Because oriented non-crystalline material cannot be studied by XRD, other methods, such as birefringence and vibrational spectroscopy, have also been used to characterize orientational amorphous and crystalline features of PET.

The aim of the work presented here was the study of a series of PET yarn samples, including both drawn as well as spin-oriented materials, in order to determine their structural and morphological characteristics by various physical methods of evaluation. The results of this series of studies are expected to provide better structure–property correlations. The Raman studies to be reported here represent a part of this overall project.

In this work we have recorded polarized Raman spectra of individual spin-oriented and drawn filaments of PET. Systematic comparison of spectra shows the development of orientation and crystallization of the polymer. By relying on band assignments of previous authors, it is possible to separate features due to molecular alignment, conformation and crystallization.

REVIEW OF RAMAN LITERATURE

Raman spectra of oriented and of crystallized PET have been reported over the last 10–15 years by several laboratories. Purvis, Bower and Ward³ were the first to show that polarization analysis of the Raman spectra of PET could yield information regarding bulk orientation of the polymer. In their study, optical birefringence correlated well with observed orientation distributions (as measured by $\cos^2\theta$ and $\cos^4\theta$).

Melveger⁴ related the Raman width of the carbonyl

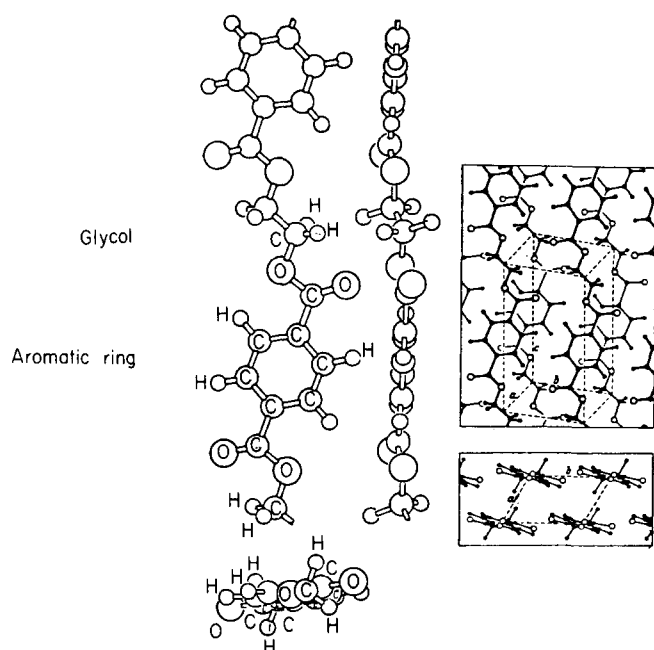


Figure 1 Molecular structure of poly(ethylene terephthalate) (PET) chain when the glycol unit is in the all-*trans* conformation and those all-*trans* chains are packed in the crystalline phase. Reproduced from a chapter by Bunn in *Fibers from Synthetic Polymers*, Figures 11.5 and 11.6, p. 295, ed. Rowland Hill (Elsevier, New York, 1953)

band to the degree of crystallinity, which could be estimated from the density of the material. The sharpening of the band in the crystalline phase was attributed to the coplanarity of the carbonyl and aromatic groups, which enables resonance stabilization of the π electrons.

Bahl *et al.*^{5a} and Boerio *et al.*^{5b} performed a normal coordinate analysis on PET utilizing a force field relevant to a family of chemically- and structurally-related aromatic polyesters, with and without deuteration. The results of this calculation were used to interpret the crystallization-induced changes observed in the i.r. and Raman spectra of PET. In addition to the sharpening of the carbonyl band, features at 1096 and 1000 cm^{-1} appear in crystalline samples but are absent in amorphous material. The band at 1096 cm^{-1} represents a combination of C–O stretching, COC bending, CCO bending and C–C stretching in the ethylene glycol segment. Choice of the assignment of the molecular motion of the 1000 cm^{-1} band between two possibilities could not be established in this article. An A_g mode (in the C_{2h} point group) was calculated near 997 cm^{-1} , arising from ethylene glycol O–CH₂ and C–C stretching motions. In addition a B_g mode was calculated to be near 995 cm^{-1} and would contain ring CH out-of-plane bending and ring torsion.

In a subsequent paper⁶ Boerio and Bailey reported polarized Raman spectra of highly oriented fibres in order to identify the symmetry characteristics of the Raman bands. Snyder⁷ had already shown that polarized Raman spectra of oriented fibres could be analysed. However, he had considered systems in which the fibre axis coincides with a symmetry axis of the polymer. In the case of PET, the C_2 symmetry axis is *perpendicular* to the molecular axis. Since the molecular axis aligns along the fibre direction, and is not a symmetry element of the polymer, Snyder's formalism cannot be applied without modification. Boerio and Bailey recognized this fact and were

able to develop the appropriate polarization analysis for PET. (More recently Schlotter and Rabolt⁸ developed a formalism for scattering in systems where the molecular symmetry axis is perpendicular to the macroscopic uniaxial direction).

Boerio and Bailey's polarized Raman data clarified the ambiguity in the normal mode assignment of the band at 1000 cm^{-1} . Since it appears with A_g symmetry, it must be assigned to O–CH₂ and C–C stretching motions of the ethylene glycol segment.

Other bands⁶, less sensitive to degree of crystallinity, also could be assigned to A_g or B_g symmetry, depending on the type of molecular motion involved. The 857 cm^{-1} band was observed to have A_g symmetry and was therefore assigned to the ring stretching mode calculated near 844 cm^{-1} . In this work only one mode with B_g symmetry was observed; its frequency was 800 cm^{-1} and was confirmed to be a band calculated at 801 cm^{-1} arising from C=O and ring-ester CC out-of-plane bending and ring torsion.

Molecular orientation was also studied by Purvis and Bower⁹, whose data indicated that, in contrast to the conclusion of Boerio and Bailey⁶, the 632 cm^{-1} band is also depolarized and would therefore arise from an asymmetric mode (B_g). Purvis and Bower used the measured degree of polarization in an attempt to choose between one of two models to describe the conformation of the amorphous polymer. Unfortunately the Raman data in combination with i.r. and optical birefringence measurements do not definitively rule out either. However, the models considered do provide a framework for visualizing the orientation and crystallization of PET that is relevant to the data to be presented in this paper.

In one model, the terephthaloyl residue is in the same conformation in amorphous and crystalline polymers and the main conformational difference between the phases is in the presence of *gauche* bonds in some of the glycol residues of the amorphous chains. The possible molecular conformations and rotational isomers have also been considered in some detail by i.r. investigators^{10–13}. Orientation factors correlated with *trans-gauche* isomerization. Garton *et al.*¹³ examined spin-oriented fibres and found a correlation between the *trans* conformation of the ethylene glycol segment and the take-up speed. In all cases the number of *gauche* bonds was observed to decrease with increasing molecular orientation.

In the second model presented by Purvis and Bower, describing amorphous PET, there are two sources of disorder of the molecular conformation. In addition to the *gauche* conformation of the glycol oxygen and carbon linkages, the presence of rotational freedom of the ring-ester C–C bond in the amorphous polymer randomizes the orientation of the plane of the ester group with respect to the aromatic plane.

Stokr *et al.*¹⁴ in fact identified Raman bands specific to particular conformers by comparison of their spectra of amorphous and dissolved PET with those of model compounds (methyl benzoate, dimethyl terephthalate, ethyl benzoate, diethyl terephthalate and ethylene glycol dibenzoate) in crystalline and liquid states.

Andersen and Muggli¹⁵ were the first to demonstrate that polarized Raman spectra of individual polymer filaments recorded on the MOLE[®] Raman microprobe reproduced accurately polarized Raman spectra recorded on bulk oriented material.

In the following series of polarized Raman spectra of spin-oriented fibres of PET recorded here, it will become clear that the orientation of the polymeric chains can be monitored independently of the crystallization, which occurs subsequently to orientation in the spin-line.

The data presented in this work were acquired from single filaments (approximately 20 μm diameter) positioned on a microscope stage where the beam waist was 1 μm and the depth of focus approximately 10 μm . Spectra of various polarization combinations from a single spot on a given fibre were acquired and intensity ratios compared to those of fibres spun under other conditions. Because these measurements were not totally analogous to those of earlier workers, it is important that the underlying rationale be described explicitly.

METHODS

Rationale of polarized Raman measurements of spin-oriented fibres

Raman scattering involves two photons, and the polarization of each can be defined. Consequently the physical parameter that determines the scattering process is the electronic polarizability, a second rank tensor which can be modulated by molecular-crystalline vibrations. From the symmetry of the system, and the symmetry of the vibrational distortions, selection rules have been derived. This means that different vibrations have distinguishable polarization behaviour^{1 6a, 1 6b}.

In a totally unoriented system, that is a liquid or a clear amorphous solid, all possible combinations of polarizations relative to orientation are accounted for in the polarization ratio, $\rho = I_{\perp}/I_{\parallel}$, where I_{\perp} and I_{\parallel} are the respective band intensities for Raman light polarized \perp (perpendicular) and \parallel (parallel) to the incident laser light. Except in unusual circumstances (such as resonance Raman conditions, electronic or spinflip scattering) I_{\perp} is always less than I_{\parallel} .

In an oriented system, the laser and Raman polarizations can be aligned along molecular-crystalline axes. In such cases it is common for certain bands to have higher intensities for off-diagonal components. In addition, in systems which are uniaxial or biaxial the diagonal intensities along different directions can be quite different.

Based on our understanding of the above we can define two criteria for detecting orientation in spin-oriented and drawn fibres of PET. In order to describe these criteria an axis system has to be defined.

Individual fibres of PET were examined on a rotating stage of the Raman microprobe. The fibre bundles were picked apart slightly before mounting on a standard microscope slide with adhesive tape, applying a minimum of tension to keep the fibres stationary. Viewed on the monitor the fibre could be accurately positioned vertically or horizontally. When the sample is mounted on a rotation stage the input laser beam, which is polarized in the horizontal direction, can be oriented along the fibre axis or perpendicular to it. The polarization of the Raman light can be chosen to be horizontal or vertical, independently of the fibre orientation.

We define the Z axis of our samples as the macroscopic fibre axis. We define an R axis as one of the radial directions (perpendicular to Z); when needed the second orthogonal axis is defined as R' . There are three inde-

pendent measurements that can be made on fibres examined radially (i.e., the fibre lies on the stage and the laser and Raman beams propagate along radial directions). From a single spot on a fibre from each sample we acquired spectra that we label ZZ , ZR and RR . The first letter indicates the laser polarization, and the second the Raman polarization. Occasionally we may also show Porto's notation: e.g. $R'(ZZ)R'$ indicates that the incident and scattered beams were propagating along R' and $-R'$ directions.

Increasing the take-up speed of spin-oriented PET fibres or increasing their draw ratio improves the degree to which the polymer axis is aligned along the fibre axis, Z . The R and Z directions will be quite different in well-oriented fibres, but indistinguishable in un-oriented samples. Thus the first criterion for orientation is inequivalence of RR and ZZ spectra of PET.

The second criterion follows the work of Boerio and Bailey⁶. These authors use polarization measurements of an oriented rod of PET to determine that the only asymmetric type vibration observed in their Raman spectrum of PET occurred at 800 cm^{-1} . It was pointed out in this article that only asymmetric modes can have higher intensities in the off-diagonal scattering than in the diagonal scattering. However, this can be observed only in highly oriented systems. So, our second criterion for orientation is a higher intensity of the asymmetric mode, such as that at 800 cm^{-1} , in the ZR spectrum rather than in the ZZ or RR spectra.

*Description of MOLE[®] Raman microprobe**

The MOLE[®] Raman microprobe used for this work is shown schematically in Figure 2. The U1000 double monochromator containing master, plane holographic gratings is optically and mechanically coupled to a metallographic microscope. Either 40 \times or 80 \times objectives with respective numerical apertures 0.85 or 0.90 were used to focus the laser beam and collect the Raman scattered radiation. A beam splitter in the nosepiece is used to disentangle the two beams. Polarization measurements were performed by placing a polarization analyser behind the microscope, and a polarization rotator behind the analyser when needed to compensate for the gratings' dichroism. The measured dichroism of the transmission of the beam splitter was less than 10%. The polarization ratio of the symmetric stretch of benzene at 992 cm^{-1} was measured as a check for accuracy; our measured value was 0.022, which compares favourably to the literature value of 0.065¹⁷. The orientation of the sample fibres was achieved by mounting fibres on a rotating microscope stage, as mentioned earlier and shown in Figure 3. A spot on a fibre was selected and then Raman spectra were recorded from that one spot with ZZ , RR and ZR (or RZ) combinations. No significant differences between RZ and ZR intensities were observed when both combinations were recorded. The minimum beam waist is no greater than 1 μm . With the field aperture open, it is assumed that signals originate across the thickness of the fibre.

Samples

Two series of PET fibres were provided by H. M. Heuvel and R. Huisman of the Enka bv Research Institute,

* The MOLE[®] Raman microprobe is manufactured by Jobin Yvon in Longjumeau, France, and Instruments SA in Metuchen, New Jersey.

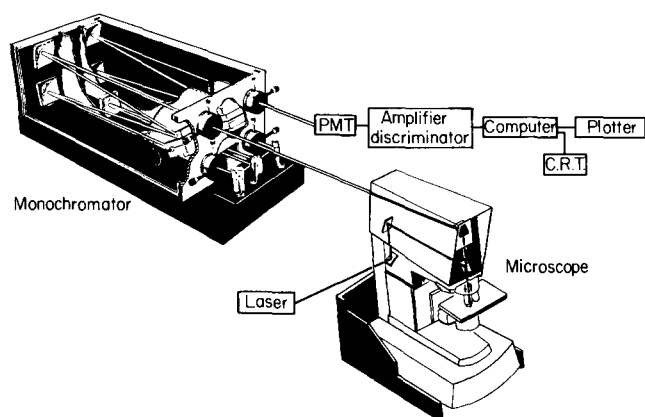


Figure 2 Schematic of the Raman microprobe MOLE¹⁸

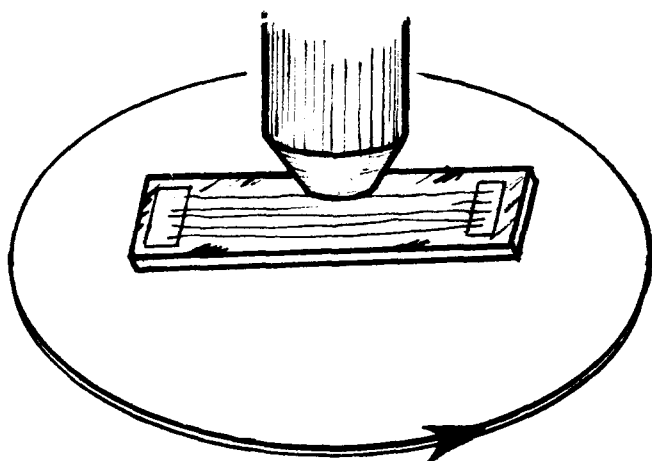


Figure 3 Schematic illustration of fibres mounted on a rotating microscope stage which enables examination of same spot on fiber with laser polarization parallel and perpendicular to fibre axis

6800 AB Arnhem, Netherlands. One series was spun to a yarn count of 165 dtex (for 30 filaments) with wind-up velocities of 1500, 2500, 3500, 4500 and 5500 m min⁻¹.

The second series was spun at a wind-up velocity of 500 m min⁻¹ and subsequently drawn to different ratios: 3.8, 4.2, 4.6 and 5.0:1 respectively. These yarns were drawn in 2 steps with pins adjusted to 90°C and 150°C.

Heuvel and Huisman also provided density measurements and X-ray diffraction evaluation (axis dimensions, crystal density of the unit cells, and crystalline orientation factors) as described in their publications¹⁸. Additionally

Otto Burkhardt (Celanese Research) measured the densities (in a calcium nitrate/water column) and a Sigrid Ruetsch (Textile Research Institute) obtained the birefringence data with an interference microscope* of these samples.

Refractive index measurements parallel and perpendicular to the filament axis were made using a Peraval Interphako transmitted light interference microscope. Interference fringes ($\lambda = 551$ nm) were generated by grating plate disk and Mach Zehnder interferometer. Fringe patterns on sheared duplicated images of the filaments mounted in a liquid of suitable refractive index differing by no more than 0.005 from that of the fibre were recorded on high speed Type 667 Polaroid film (ASA 3000). In addition a fibre sample that had been spin-oriented at 1500 m min⁻¹ was drawn at room temperature to a maximum draw-ratio of about 2.5:1 and was characterized by X-ray diffraction and birefringence. Its wide angle X-ray diffraction pattern (obtained with nickel-filtered CuK α radiation) is shown in Figure 4. The averaged measured birefringence was 121×10^{-3} . All data are collected in Table 1.

Table 1 shows that the densities, unit cell dimensions, crystallinities, birefringences and crystalline orientation factors of the four drawn samples are very similar, the crystallinity being about 30%. For the spin-oriented materials, only the samples with wind-up velocities of 4500 and 5500 m min⁻¹ are crystalline on the basis of X-ray diffraction data; while the crystalline orientation functions are as high as for the drawn materials, their % crystallinity is lower. The overall orientation for the drawn samples is high, as shown by the high value of the birefringences. The spin-oriented samples show a gradual increase in birefringence with take-up velocity to a considerably lower maximum value than for drawn fibres. This is generally observed for spin-oriented polyethylene terephthalate fibres¹⁹ and indicates considerably lower orientation in the non-crystalline regions of this type of PET fibre. (The highest birefringence value observed for a sample prepared by this process at a take-up velocity of 7000 m min⁻¹ is 150×10^{-3} (ref. 19c).)

* The interference microscope was manufactured by Jenoptik Jena Inc., German Democratic Republic, and supplied by Martin Instrument Co., Greenville, SC.

Table 1 Characterization of PET samples

Sample no.	History	Density ^a g cm ⁻³	Density ^b g cm ⁻³	Birefringence ^c × 10 ³	<i>a</i> axis (Å)	<i>b</i> axis (Å)	<i>c</i> axis (Å)	Crystal density	% Crystallinity	<i>f</i> _c	
	500 m min ⁻¹ TUS										
1	D.R = 5.0	1.3817	1.3786	213.0	4.520	5.926	10.710	1.477	26.9 ^d	29.2 ^e	0.97
2	D.R = 4.6	1.3820	1.3825	203.9	4.539	5.932	10.715	1.468	31.7 ^d	31.4 ^e	0.97
3	D.R = 4.2	1.3802	1.3822	207.7	4.532	5.915	10.693	1.478	29.5 ^d	28.4 ^e	0.96
4	D.R = 3.8	1.3800	1.3815	205.0	4.533	5.920	10.683	1.476	29.1 ^d	28.8 ^e	0.95
5	1500 m min ⁻¹ TUS	1.3368	1.3385	11.2	—	—	—	—	—	—	—
5'	D.R. = 2.5:1 (RT)			121	—	—	—	—	—	—	—
6	2500 m min ⁻¹ TUS	1.3386	1.3392	24.9	—	—	—	—	—	—	—
7	3500 m min ⁻¹ TUS	1.3420	1.3429	47.3	—	—	—	—	—	—	—
8	4500 m min ⁻¹ TUS	1.3517	1.3536	75.2	4.551	5.994	10.710	1.454	11.1 ^d	9.1 ^e	0.96
9	5500 m min ⁻¹ TUS	1.3771	1.3784	107.4	4.485	5.906	10.698	1.495	23.7 ^d	22.6 ^e	0.98

^a Measured by O. Burkhardt, Celanese Corp., USA

^b Measured by Heuvel and Huisman at Enka

^c Measured by Sigrid Ruetsch at Textile Research Institute

^d % crystallinity based on data of a

^e % crystallinity based on data of b

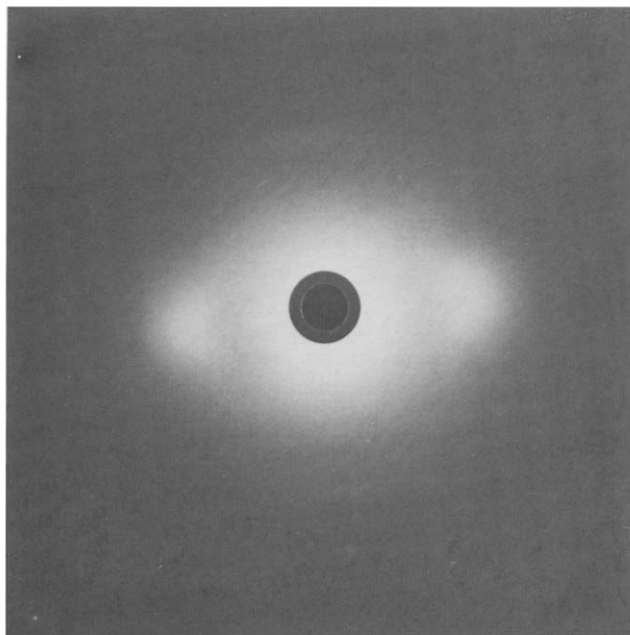


Figure 4 X-ray diffraction pattern of sample No. 5' (spin-oriented at 1500 m min^{-1} and drawn at room temperature with a ratio of ca. 2.5:1)

RESULTS

Figure 5 presents polarized Raman spectra from a single point in a fibre spun at 1500 m min^{-1} (sample 5). Spectra from the ZZ, ZR and RR polarization combinations are presented. The vertical intensity scales have been normalized to enable comparison of intensities between the three scans. Absolution intensities were reproducible to 15%. Within this 15% variability, the ZZ and RR spectra are indistinguishable. All bands in the ZR spectrum, except for the 632 and 800 cm^{-1} bands, are diminished in intensity; the intensities of these bands are comparable to those of the diagonal spectra.

Figure 6 reproduces similar spectra from a point on a fibre spun at 5500 m min^{-1} . In this case the RR intensity is significantly reduced relative to that of the ZZ spectrum. In the off-diagonal (ZR) spectrum all bands, except those at 632 and 800 cm^{-1} , show intensities lower than those in the ZZ or RR spectra.

The comparable or stronger intensities of the 632 and 800 cm^{-1} bands in the ZR spectra relative to their intensities in ZZ or RR scans confirm these bands to have B_g , rather than A_g , character.

The intensity ratios of the major bands have been calculated and tabulated in Table 2. Since the intensities are considered to be reproducible to $\pm 15\%$, there will be $\approx \pm 30\%$ uncertainty in the ratios as calculated from these spectra ($0.85/1.15 = 0.75$, $1.15/0.85 = 1.35$). These numbers are presented as typical for a series of scans recorded, not necessarily definitive.

The development of orientation can be monitored by examining the trends in the intensity ratios as a function of take-up speed. For instance $I_{RR}:I_{ZZ}$ of the 1615 cm^{-1} band decreases from approximately 1.1 to 0.1 in the series of fibres examined. Other bands exhibit similar decreases in $I_{RR}:I_{ZZ}$. As described earlier, the inequivalence of the macroscopic Z and R axes is consistent with alignment of the molecular axes during spinning and/or drawing.

These data record the development of orientation in these fibres on the basis of polarization intensity ratios. In

addition, changes in molecular alignment and interchain packing of polymer units can be monitored by the appearance and disappearance of several bands. The literature cited earlier shows that conformational and/or packing changes of the glycol units can be observed in bands in the $900\text{--}1200 \text{ cm}^{-1}$ range. Spectra recorded in this region are shown in Figure 7. All fibres have well-defined bands at 1120 and 1175 cm^{-1} . Fibres spun at low take-up speeds consistently show weak, poorly defined features at about 1030 and 1100 cm^{-1} . As the take-up speed is increased, the diffuse band at 1030 cm^{-1} is replaced by a well-defined, relatively sharp band at 1000 cm^{-1} . (The 1000 cm^{-1} band is highly polarized, appearing only in the ZZ spectrum of 'crystalline' fibres.) In addition, the shoulder in the 1100 cm^{-1} range becomes the most intense, sharpest band (1096 cm^{-1}) in this region of the spectrum. Both bands have been correlated with 'crystallinity' in PET^{5,6,14}.

Crystallization has also been correlated with the width of the carbonyl band at 1730 cm^{-1} . Previously Melveger⁴

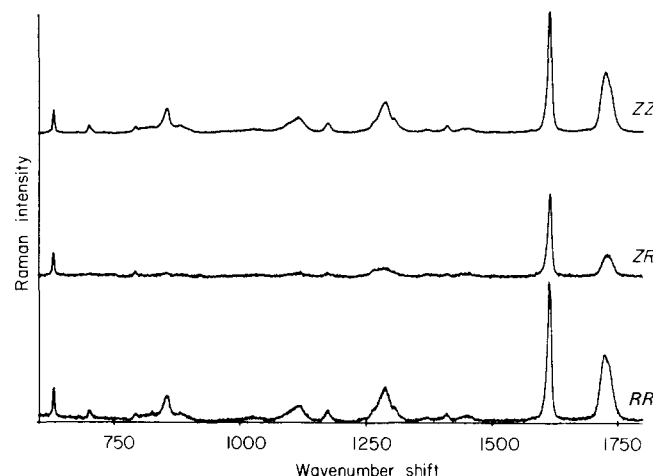


Figure 5 Polarized Raman spectra between 600 and 1800 cm^{-1} of a single $20 \mu\text{m}$ fibre of poly(ethylene terephthalate) spin-oriented at 1500 m min^{-1} . Laser intensity was 2.5 mW at the sample. Spectra have been displayed so that relative intensities represent scattering intensity differences due to polarization differences. ZZ(RR) indicates that the laser and Raman polarization were parallel (perpendicular) to the fibre axis; ZR indicates that laser polarization was parallel to the fibre axis and the Raman polarization was perpendicular to the fibre axis. Differences in signal to noise ratios arise from differences in integration times which have been normalized in the plotted intensities

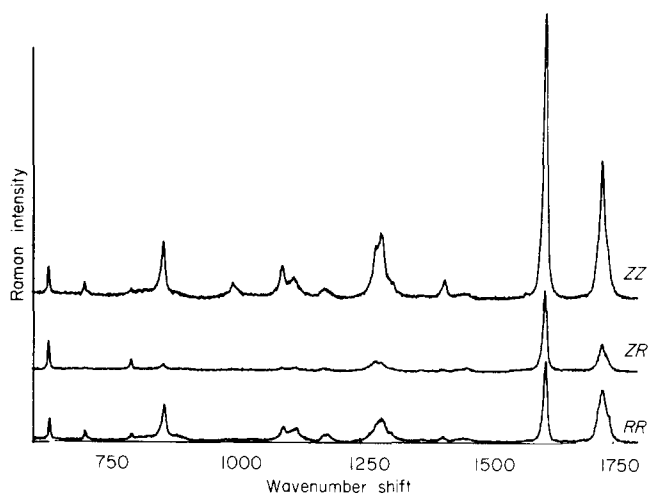


Figure 6 Polarized Raman spectra of a single $20 \mu\text{m}$ fibre of PET spin-oriented at 5500 m min^{-1} . Laser intensity was 4 mW at the sample. All other comments in Figure 5 apply

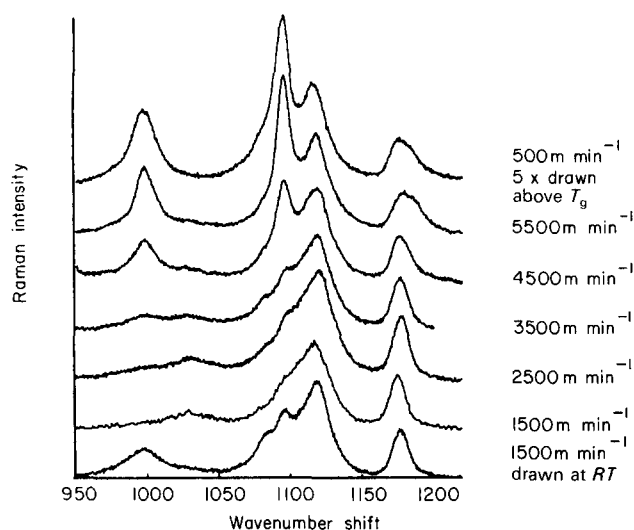


Figure 7 ZZ component of the Raman spectra between 950 and 1220 cm^{-1} of five samples spin-oriented with take-up speeds (TUS) 1500, 2500, 3500, 4500 and 5500 m min^{-1} and two drawn samples. The spectrum at the top of the Figure was recorded from a fibre spin-oriented at 500 m min^{-1} and drawn 5 \times over pins held at 90 and 150°C; the spectrum at the bottom of the Figure was recorded from a fibre spin-oriented at 1500 m min^{-1} and drawn 2.5 \times at room temperature

had shown a correlation between the density of a PET sample and the half-width of the carbonyl band at 1725–1730 cm^{-1} . Stokr *et al.*¹⁴ had indicated that in the crystalline state, in addition to being coplanar with the aromatic ring, the carbonyl groups are in *trans* conformation to each other; however, in the amorphous state the carbonyl groups can be randomly arranged with respect to the aromatic ring and to one another.

Figures 8a–c and Table 3 give some of the preliminary data of the 1725–1730 cm^{-1} band for samples 5, 9 and 1 for ZZ, ZR=ZR and RR polarization. The spectra are displayed with Y axis expansions which give equivalent maximum intensities to each spectrum. The differences in the shape of the bands for each fibre indicate that the carbonyl bands represent a multiplicity of conformations, which will have to be analysed by curve-resolving techniques. Most clearly this is shown for the amorphous sample No. 5, which shows three maxima at 1721, 1726 and 1731 cm^{-1} . While the crystalline samples have one main peak at 1725 cm^{-1} , it is clear that the other two components are present there also (1730 cm^{-1} in the ZR and 1721 cm^{-1} in the RR spectra). The half-width data reported here fit the Melveger⁴ correlation with density. The peak intensity ratios (I_{ZR}/I_{ZZ} and I_{RR}/I_{ZZ}) are listed in Table 2.

Implicit in most previous Raman studies of oriented PET is the coupling of orientation and crystallization. This is due to the fact that preparation of the materials used by these authors, be it fibre or film, involved orientation by drawing of the unoriented material at or above the glass-transition temperature (T_g) and, therefore, simultaneously produced crystallization. Obviously, in these drawing processes, the degree of orientation can be changed by adjusting the draw-ratio, while the crystallinity can be modified by changing the drawing temperature, the number of drawing steps and the annealing conditions of the drawn product. Normally this drawing process leads to samples where orientation and crystallization occur simultaneously.

In contrast, the spin-orientation process can lead to materials with a range of orientations, some of the fibres being amorphous, others partially crystalline (as determined by wide angle X-ray diffraction methods), depending on spinning conditions (yarn take-up, spin stress, extrusion temperature, polymer molecular weight, etc.)¹⁸. Thus, for example, some PET yarns spun by this method in a range of take-up speeds between 1500–3500 m min^{-1} (so-called POY materials: Partially Oriented Yarns) show increasing orientation but are all amorphous. Yarns spun at or above 4000 m min^{-1} take-up speed (4000–10000 m min^{-1}) are usually crystalline and have highly oriented crystalline areas. Again, the amount of crystalline material depends on spinning and annealing conditions.

The data presented here show the spectra of a few spin-oriented fibres of gradually increasing orientation (take-up speeds 1500–3500 m min^{-1}) which are amorphous by X-ray diffraction, two spin-oriented samples (take-up speed 4500 and 5500 m min^{-1}) which show high crystalline orientation and different degrees of crystallinity, and a doubly drawn PET yarn (90+150°C), highly oriented

Table 2a Peak height ratios, I_{RR}/I_{ZZ}

$\Delta\tilde{\nu}$ (cm^{-1})	Sample No.						
	5	6	7	8	9	1	5' drawn
632	1.3	1.0	0.6	1.0	0.8	0.7	0.8
704	1.1	0.9	0.7	0.7	0.8	0.8	0.9
797	1.1	1.93	0.8	0.9	1.1	0.8	0.8
850, br.amorph.	0.9	0.7	0.5	0.8	1.0	1.4	1.1
858	0.9	0.8	0.6	0.8	0.6	0.6	0.5
999	—	—	—	0.0	0.1	0.0	0.0
1030	1.7	1.2	?	—	—	—	2
1096	—	—	0.6	0.5	0.5	0.5	0.5
1117	0.9	0.8	0.6	0.7	0.7	0.6	0.5
1177	1.3	0.9	0.6	0.8	0.9	1.0	0.8
1293	1.1	0.7	0.4	0.5	0.4	0.3	0.3
1371	1.7	0.7	0.7	1.3	—	—	—
1419	1.0	0.6	0.4	0.4	0.3	0.2	0.2
1453	1.2	0.9	0.6	0.9	0.9	0.5	0.5
1615	1.1	0.7	0.4	0.4	0.3	0.1	0.2
1729	1.1	0.7	0.5	0.5	0.4	0.3	0.4

Table 2b Peak height ratios: I_{ZR}/I_{ZZ}

$\Delta\tilde{\nu}$ (cm^{-1})	Sample No.						
	5	6	7	8	9	1	5' drawn
632	1.1	1.0	1.1	1.6	1.1	1.1	1.3
704	0	0	0.2	0.1	0.1	0.1	0
797	1.5	1.2	1.8	2.1	2.5	2.2	1.8
850, br. amorph.	0.2	0.2	0.2	0.1	0.2	0	0.3
858	0.1	0.1	0.1	0.2	0.1	0.1	0.1
999	—	—	—	0.1	0	0.3	0.1
1030	0.7	1.0	—	—	—	—	—
1096	—	—	0.2	0.1	0.1	0.1	0.1
1117	0.2	0.2	0.2	0.2	0.2	0.2	0.1
1177	0.3	0.3	0.3	0.3	0.4	0.3	0.4
1293	0.3	0.3	0.2	0.2	0.2	0.1	0.2
1371	1.3	0.4	0.9	1.3	—	0.2	—
1419	0.4	0.3	0.3	0.3	0.1	0.1	0.2
1453	0.7	0.9	1.0	1.0	0.9	0.4	0.6
1615	0.7	0.6	0.5	0.5	0.3	0.2	0.2
1729	0.3	0.3	0.3	0.3	0.2	0.2	0.2

These data were collected with 1 point/ cm^{-1} and 300 μm slits (optical resolution $\approx 3 \text{ cm}^{-1}$).

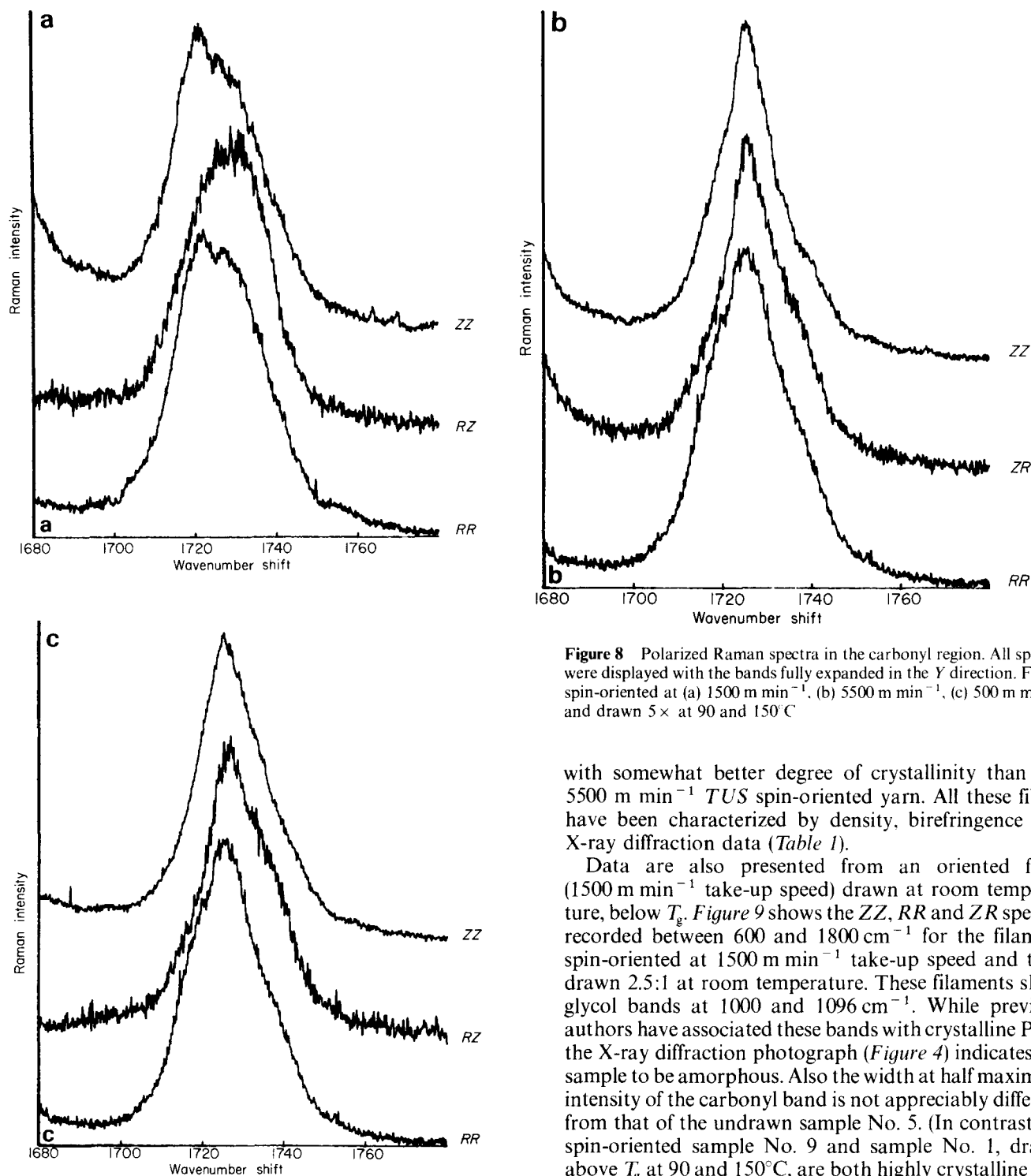


Figure 8 Polarized Raman spectra in the carbonyl region. All spectra were displayed with the bands fully expanded in the Y direction. Fibres spin-oriented at (a) 1500 m min⁻¹, (b) 5500 m min⁻¹, (c) 500 m min⁻¹ and drawn 5× at 90 and 150°C

with somewhat better degree of crystallinity than the 5500 m min⁻¹ TUS spin-oriented yarn. All these fibres have been characterized by density, birefringence and X-ray diffraction data (Table 1).

Data are also presented from an oriented fibre (1500 m min⁻¹ take-up speed) drawn at room temperature, below T_g . Figure 9 shows the ZZ, RR and ZR spectra recorded between 600 and 1800 cm⁻¹ for the filament spin-oriented at 1500 m min⁻¹ take-up speed and then drawn 2.5:1 at room temperature. These filaments show glycol bands at 1000 and 1096 cm⁻¹. While previous authors have associated these bands with crystalline PET, the X-ray diffraction photograph (Figure 4) indicates the sample to be amorphous. Also the width at half maximum intensity of the carbonyl band is not appreciably different from that of the undrawn sample No. 5. (In contrast the spin-oriented sample No. 9 and sample No. 1, drawn above T_g at 90 and 150°C, are both highly crystalline and

Table 3 Data for carbonyl bands

Sample	ZZ		ZR or RZ		RR		Relative intensity	
	FWHM ^a	Freq. ^b	FWHM	Freq.	FWHM ^a	Freq. ^b	ZR:ZZ	RR:ZZ
No. 1	18	1725	19	1724.6	19	1724.6	0.2	0.2
No. 9	13	1725.3	15	1725.1	19	1724.8	0.2	0.2
No. 5	24	1721.4	24	1726.0	25	1721.1	0.4	1.02
		1725.1		1731.1		1727.4		
		1730.1						
No. 5'	27	1722.8	24	1728.3	24	1731.7	0.3	0.6
		1728.3						

^aFWHM=full width at half maximum intensity

^bFreq.=Raman frequency in cm⁻¹

These data were collected with 5 points/cm⁻¹ and 300 m slits (optical resolution ca. 3 cm⁻¹)

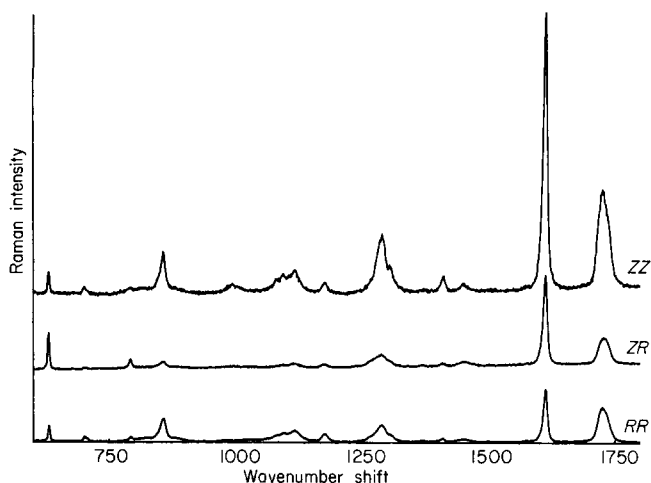


Figure 9 Polarized Raman spectra between 600 and 1800 cm^{-1} of a single fibre of polyethylene terephthalate spin-oriented at 1500 m min^{-1} and drawn at room temperature to a ratio of 2.5:1. Laser intensity at sample was 4 mW. All other comments from Figure 5 apply

their carbonyl linewidths are narrower than those of sample No. 5.) The X-ray photograph, the high birefringence and the Raman intensity ratios of sample No. 5 drawn at room temperature (No. 5') indicate very good orientation of the polymer chains.

A comment regarding the band at 1080 cm^{-1} should be made. Careful inspection of the spectra of all the fibres reveals a more or less intense shoulder in this region. The shoulder is very strong in the room-temperature drawn fibre (No. 5') and is also clearly present in fibres No. 1 (drawn at 90 and 150°C) and No. 7 (spin-oriented at 3500 m min^{-1} TUS). It is least visible in fibre No. 9 (spin-oriented at 5500 m min^{-1}). It is our feeling that this band correlates with an aligned glycol unit in the amorphous phase, representing one of the conformations described by Stokr *et al.*¹⁴.

As has been reported by Stokr¹⁴ and Ward and Wilding²⁰ the shift of the band from 1175 to 1182 cm^{-1} in the presence of adequate crystallinity accounts for the broadening of this peak in the 5500 m min^{-1} , and 500 m min^{-1} 5 \times drawn samples (Nos. 9 and 1 respectively). Thus the 1182 cm^{-1} band seems to be a true crystallinity band.

A final comment can be made regarding a broad Raman band in the region between 800 and 900 cm^{-1} in the ZZ and RR spectra. We have attributed it to scattering by the amorphous component of these samples and subtracted its intensity from the peak heights of the 800 and 860 cm^{-1} bands listed in Table 2. This background is practically absent in the ZR spectrum. In earlier work²¹ we observed a considerably stronger intensity of this background with Raman spectra excited axially (laser and Raman beams propagating parallel to the fibre axis) rather than radially (as carried out here).

DISCUSSION

Previous investigations of the Raman spectra of PET and sometimes other polyesters dealt either with amorphous and crystalline (semicrystalline) unoriented materials or they dealt with oriented materials which because of their method of preparation (drawing above T_g) of necessity were crystalline materials. The Raman spectrum of an oriented, non-crystalline material does not seem to have been investigated in detail. (Purvis, Bower and Ward³

examined a cold-drawn film and correlated the Raman orientation factors of only the 1616 cm^{-1} band with its optical birefringence.)

The i.r. spectra of POY PET samples have been reported by Garton *et al.*¹³. They investigated samples, spin-oriented at 2000–3500 m min^{-1} take-up speed. The samples ranged in birefringence from 18 to 49×10^{-3} , with densities of 1.341 to 1.344 g cm^{-3} and a *trans*-index (a measure of the concentration of the *trans* conformation in the glycol unit) of 1.34 to 1.84. All of Garton's samples were non-crystalline, as are our samples between 1500 and 3500 m min^{-1} take-up speed.

I.r. absorption bands allow measurements of *trans* and *gauche* conformations of the glycol units^{10–13}. X-ray diffraction data (Daubeny *et al.*¹) have shown that the crystalline arrangement of the polymer chain requires a *trans*-conformation of the glycol units in the crystal, and a *trans*-arrangement of the carbonyl groups as well as their co-planarity with a benzene ring.

In the non-crystalline state, the co-planarity and *trans*-conformation of the carbonyl groups is not required and the *gauche* conformation in the glycol unit is prevalent. However, some *trans*-conformation of this unit seems to be present even in unoriented amorphous PET (approximately 10%)¹³. Thus it is essential to be able to differentiate *trans*-conformations in various environments—i.e., in the amorphous or in the crystalline regions. Only the intensity of the latter should correlate with X-ray crystallinity. Both Stokr¹⁴ and D'Esposito¹² show that there are slight shifts in the position of the i.r. *trans* absorption bands in the amorphous and crystalline phases. Also, since not all the bands involving the glycol and carbonyl groups have to have the *trans* conformation in the non-crystalline regions¹⁴, the mutual exclusion of bands in Raman and infra-red due to the presence of a centre of symmetry is not valid and identical bands may appear in both spectra²².

The Raman peaks measured between 900 and 1220 cm^{-1} correlate with conformational changes and inter-chain effects rather than amorphous–crystalline differences. Both the 1000 and 1096 cm^{-1} bands appear in the spectrum of the amorphous sample spin-oriented at 3500 m min^{-1} . In the other spectra their intensities increase with TUS. Their intensities are also quite clear in the spectrum of the 1500 m min^{-1} fibre drawn at room temperature. The behaviour of the 1030 cm^{-1} band fits the Stokr¹⁴ assignment to a *gauche* structure of the glycol group. Its replacement by a band at 1000 cm^{-1} in the *trans* form is also consistent with the polarization orientation behaviour. Extended polyester chains require the *trans* conformation in the glycol units. Our data show the 1000 cm^{-1} band only in ZZ spectra of oriented fibres. The 1030 cm^{-1} band, however, appears in ZZ as well as RR traces (refer to Figures 3 and 4). Taken together these observations imply simultaneous occurrence of the *trans* conformation and chain orientation.

The splitting of the 1175 cm^{-1} band (ring in-plane C–H bend and C–C stretch^{5a}) into two bands at 1175 and 1182 cm^{-1} for the most crystalline samples (samples 1 and 9) seems to confirm the shift of this band due to the change in its environment¹⁴ (i.e., the arrangement of the C=O groups or aromatic ring interactions in the crystalline state).

Finally there is the shoulder at 1080 cm^{-1} visible in all spin-oriented fibres but most clearly seen in the spectrum

of the fibre spun at 1500 m min^{-1} and drawn at room temperature. The major difference between drawn and spin-oriented fibres is the concentration of load bearing, stressed chain structures (*trans* glycol conformations?) in the non-crystalline regions. Such structures should be important in *amorphous spin-oriented* and in *crystalline drawn* samples. The stressed amorphous *trans* glycol conformation should be less important in crystalline spin-oriented structures that have low amorphous orientation factors as indicated by low birefringences compared to drawn fibres. Obviously more work is required for the confirmation of the proposal that the 1080 cm^{-1} band reflects stressed *trans* glycol units in amorphous regions. Comparison of tensile data with Raman spectra (especially curve resolving of the 1100 cm^{-1} region to obtain relative intensities of the 1080 , 1096 and 1120 cm^{-1} bands) may elucidate this concept.

ACKNOWLEDGEMENTS

The authors wish to thank Drs Heuvel and Huisman (Enka, Holland) for providing the samples and some of their physical characterization. We also thank Sigrid Ruetsch (TRI) for her birefringence measurements and Otto Burkhardt (Celanese) for the density data.

REFERENCES

- 1 Daubeny, R., Bunn, C. W. and Brown, C. J. *Proc. Roy. Soc.* 1954, **226**, 531
- 2 See for example, Billmeyer, Jr, F. W. 'Textbook of Polymer Science, 2nd Edn.', Wiley Interscience, New York, 1971
- 3 Purvis, J., Bower, D. I. and Ward, I. M. *Polymer* 1973, **14**, 398
- 4 Melveger, A. J. *J. Polym. Sci. A-2* 1972, **10**, 317
- 5a Bahl, S. K., Cornell, D. D., Boerio, F. J., McGraw, G. E. *J. Polym. Sci., Polym. Lett. Edn.* 1974, **12**, 13
- 5b Boerio, F. J., Bahl, S. K. and McGraw, G. E. *J. Polym. Sci., Polym. Phys. Edn.* 1976, **14**, 1029
- 6 Boerio, F. J. and Bailey, R. A. *J. Polym. Sci., Polym. Lett. Edn.* 1974, **12**, 433
- 7 Snyder, R. G. *J. Mol. Spectrosc.* 1971, **37**, 353
- 8 Schlotter, N. E. and Rabolt, J. F. *Polymer* 1984, **25**, 165
- 9 Purvis, J. and Bower, D. I. *J. Polym. Sci., Polym. Phys. Edn.* 1974, **14**, 1461
- 10 Miyake, A. *J. Polym. Sci.* 1959, **38**, 479
- 11 Cunningham, A., Ward, I. M., Willis, H. A. and Zichy, V. *Polymer* 1974, **15**, 749
- 12 D'Esposito, L. and Koenig, K. L. *J. Polym. Sci., Polym. Phys. Edn.* 1976, **14**, 1731
- 13a Garton, A., Carlsson, D. T., Holmes, L. L. and Wiles, D. N. *J. Appl. Polym. Sci.* 1980, **25**, 1505
- 13b Garton, A., Carlsson, D. J. and Wiles, D. N. *Text Res. J.* 1981, **51**, 28
- 14 Stokr, J., Schneider, B., Doskocilova, D., Lovy, J. and Sedlacek, P. *Polymer* 1982, **23**, 714
- 15 Andersen, M. E. and Muggli, R. Z. *Anal. Chem.* 1981, **53**, 1772
- 16a Tadakoro, H. 'Structure of Crystalline Polymers', Wiley-Interscience, New York, 1979
- 16b Siesler, H. W. and Holland-Moritz, K. in 'Infrared and Raman Spectroscopy of Polymers', Marcel Dekker, Inc., New York, 1980
- 17 Porto, S. P. S. *J. Opt. Soc. Am.* 1966, **56**, 1585
- 18a Huisman, R. and Heuvel, H. M. *J. Appl. Polym. Sci.* 1978, **22**, 943
- 18b Heuvel, H. M. and Huisman, R. *J. Appl. Polym. Sci.* 1978, **22**, 2229
- 19a Frankfort, H. R. E. and Knox, B. H., US Patents Nos 4 134 882 (1979) and No. 4 195 051 (1980)
- 19b Garg, S. K. *J. Appl. Polym. Sci.* 1982, **27**, 2857
- 19c Dietrich, W., Reichelt, G. and Renkert, H. 'Chemiefasern/Text.-ind', p. 612, Sept. 1982
- 20 Ward, M. and Wilding, M. A. *Polymer* 1977, **18**, 327
- 21 Adar, F. and Noether, H. in 'Microbeam Analysis--1983', (Ed. R. Gooley), San Francisco Press, 1983, p. 269
- 22 Liang, C. V. and Krimm, S. *J. Mol. Spectr.* 1959, **3**, 554